

# Is Adversarial Training with Compressed Datasets Effective?

Tong Chen, Raghavendra Selvan

Department of Computer Science, University of Copenhagen, Denmark

{toch,raghav}@di.ku.dk

## Abstract

Dataset Condensation (DC) refers to the recent class of dataset compression methods that generate a smaller, synthetic, dataset from a larger dataset. This synthetic dataset retains the essential information of the original dataset, enabling models trained on it to achieve performance levels comparable to those trained on the full dataset. Most current DC methods have mainly concerned with achieving high test performance with limited data budget, and have not directly addressed the question of adversarial robustness. In this work, we investigate the impact of adversarial robustness on models trained with compressed datasets. We show that the compressed datasets obtained from DC methods are not effective in transferring adversarial robustness to models. As a solution to improve dataset compression efficiency and adversarial robustness simultaneously, we propose a novel robustness-aware dataset compression method based on finding the Minimal Finite Covering (MFC) of the dataset. The proposed method is (1) obtained by one-time computation and is applicable for any model, (2) more effective than DC methods when applying adversarial training over MFC, (3) provably robust by minimizing the generalized adversarial loss. Additionally, empirical evaluation on three datasets shows that the proposed method is able to achieve better robustness and performance trade-off compared to DC methods such as distribution matching.

## 1 Introduction

Deep learning (DL) has enabled large strides of progress across multiple application domains (LeCun et al., 2015; Schmidhuber, 2015). Scaling up model sizes and datasets have shown to be of import to make some of these breakthroughs (Kaplan et al., 2020; Alabdulmohsin et al., 2022). The energy consumption, and the corresponding carbon footprint, of using these large model sizes and datasets are also of a growing concern within the community (Strubell et al., 2020; Anthony et al., 2020).

Improving the environmental sustainability of DL, in particular by reducing their energy consumption, has been primarily addressed with a focus on improving the resource efficiency of DL models (Bartoldson et al., 2023). For instance, using a smaller model to condense a larger model with knowledge distillation has shown to be quite effective in reducing the energy consumption at inference (Hinton et al., 2014). Similarly, a recent class of methods has attempted to condense large datasets into smaller, synthetic, datasets under the umbrella term of *dataset distillation* or *dataset condensation* (DC) (Zhao et al., 2021). These DC methods incur a one-time cost for dataset compression, which can then be used to train multiple models or perform iterative optimization efficiently (Cui et al., 2022).

On the other hand, fairness, privacy, and robustness of DL models are also important considerations. These factors can be viewed to constitute the *social sustainability* axis (Bender et al., 2021; Kaack et al., 2022). Consider robustness as a case in point; DL models are known to be vulnerable to tiny perturbations of inputs which was first investigated using adversarial examples (Goodfellow et al., 2015). Robustness to such adversarial attacks is an important and desirable property of DL models, which otherwise makes them unreliable and unsafe when applied in various real-life applications, such as autonomous car and aerospace.

The interplay between performance, efficiency, and social sustainability aspects, is not fully understood (Wright et al., 2023). It has been shown that there is first a trade-off between performance and optimizing for social sustainability. For instance, adversarial robustness is achieved at the expense of test performance (Tsipras et al., 2019). Another level of trade-off exists between optimizing for efficiency and performance (Selvan et al., 2023). Finally, there is also a trade-off between efficiency

and social sustainability, for instance, compressed models have shown to be less fair (Hooker et al., 2020; Stoychev and Gunes, 2022).

In this work, we study the trade-off between using compressed datasets, that can improve efficiency, and their impact on the robustness of models by answering the question: **Can we improve data efficiency and robustness simultaneously?** In particular, we will focus on the distribution matching (DM) method (Zhao and Bilen, 2023) as the representative DC method, due to its inherent efficiency and superior dataset distillation capabilities compared to other DC methods. And to study robustness, we focus on adversarial training using projected gradient descent (PGD) attack based on (Madry et al., 2018), where one minimizes the average of *the worst-case loss* instead of the average loss as in the standard training, which leads to a non-convex min-max problem.

These choices result in us investigating the adversarial robustness of models trained with compressed datasets obtained from the DM method. Based on our observations, we propose a novel, *robustness-aware dataset compression* method with provable guarantees, which ensures that adversarial training with the compressed dataset is more effective than with DC methods. Our key contributions in this work are summarized below:

1. To the best of the authors knowledge, the **first** systematic study into the effectiveness of adversarial training with synthetic, compressed datasets obtained from DC methods.
2. Propose a **novel** robustness-aware dataset compression method based on minimal finite covering (MFC), which incurs a one-time computation cost, and can be applied to any models and downstream tasks.
3. Formulate MFC as a **mixed integer linear programming (MILP)**, whose upper bound or exact solution can be found using existing solvers and is better than the  $\varepsilon$ -greedy algorithm in (Sener and Savarese, 2018).
4. Present a general adversarial training framework when using a proper covering of the dataset, such that the generalized adversarial loss over the coreset serves as a **provable upper bound** of that over the original dataset.
5. Using experiments on three datasets, we empirically show that the proposed **MFC method performs better** than DM method in terms of robustness and is also competitive in terms of test accuracy.

## 2 Related Works

**Adversarial robustness:** With the emergence of adversarial attacks (Goodfellow et al., 2015), understanding and enhancing adversarial robustness have become challenging open problems. Numerous strategies for neural networks to defend against adversarial attacks have been proposed since the last decade, including randomized smoothing (Cohen et al., 2019), adversarial training (Tramèr et al., 2018), certified training (Mirman et al., 2018), and gradient norm regularization (Finlay and Oberman, 2021). RobustBench, a benchmarking platform, offers a comprehensive overview of various adversarial training methods tailored to diverse datasets and norm specifications (Croce et al., 2020).

While adversarial training has proven crucial for enhancing robustness, it only provides an intuitive understanding of downstream performance. Consequently, the research community is also seeking for methods that provide a provable guarantee of robustness. These works are usually referred to as *certified training*, which are usually more computationally expensive than adversarial training, but hold particular significance in specific applications. Popular works include interval bound propagation (Gowal et al., 2018; Zhang et al., 2019a; Mueller et al., 2023), linear relaxation (Zhang et al., 2018), semidefinite relaxation (Raghunathan et al., 2018), differential privacy (Lecuyer et al., 2019), and diffusion de-noised smoothing (Carlini et al., 2023).

**Robustness-aware model compression:** The computational expense and inefficiency associated with solving non-convex min-max problems, particularly given the large scale of datasets, pose challenges for adversarial training. Currently, the primary methods of improving the efficiency of adversarial robustness is in terms of compressed models, as shown in works such as adversarial robust

distillation (Goldblum et al., 2020) and robust model compression (Ye et al., 2019; Gui et al., 2019). These methods are based on jointly training a smaller model while preserving the adversarial robustness.

**Dataset compression:** At a high-level dataset compression methods can be categorized into two: coreset selection, and DC. Coreset selection methods select a subset with representative samples from the original dataset and include classic techniques such as K-center selection (Farahani and Hekmatfar, 2009) and herding (Chen, 2009; Chen et al., 2010).

DC methods are used to generate a smaller set of synthetic data from the larger original dataset so that a model trained on the smaller dataset yields the same performance as when trained with the original dataset. The original DC method introduced in Wang et al. (2018) synthesized new data by matching performance to a network trained with the original dataset. Further methods have been developed for DC by matching gradients (Zhao et al., 2021), training trajectories (Cazenavette et al., 2022), and intermediate feature-maps (Wang et al., 2022). While these DC methods match some form of performance based on some explicit downstream task, distribution matching (DM) introduced in (Zhao and Bilen, 2023) performs DC by matching the statistics of the original and the synthetic distributions in a learnt embedding space (which implicitly could correspond to the downstream task). An overview of more recent methods is presented along with benchmarking in (Cui et al., 2022).

### 3 Preliminaries and Notations

Consider the  $n$ -dimensional Euclidean space  $\mathbb{R}^n$  with norm  $\|\cdot\|$ . In particular, for  $p > 0$ , the  $\ell_p$ -norm over  $\mathbb{R}^n$  is defined as  $\|\mathbf{x}\|_p = (\sum_{i=1}^n |x_i|^p)^{1/p}$  if  $p < \infty$  and  $\|\mathbf{x}\|_p = \max_i |x_i|$  if  $p = \infty$ . Define a distance metric  $d(\mathbf{x}, \mathbf{y}) = \|\mathbf{x} - \mathbf{y}\|$  for any two points  $\mathbf{x}$  and  $\mathbf{y}$  in  $\mathbb{R}^n$ . Given a point  $\mathbf{x}$  and a dataset  $\mathcal{Y}$ , the distance between  $\mathbf{x}$  and  $\mathcal{Y}$  is the infimum of distances between  $\mathbf{x}$  and all points in  $\mathcal{Y}$ , which is given by  $d(\mathbf{x}, \mathcal{Y}) := \inf_{\mathbf{y} \in \mathcal{Y}} d(\mathbf{x}, \mathbf{y})$ , and the distance between two datasets is defined as  $d(\mathcal{X}, \mathcal{Y}) := \inf_{\mathbf{x} \in \mathcal{X}} \inf_{\mathbf{y} \in \mathcal{Y}} d(\mathbf{x}, \mathbf{y})$ . The (quasi)-distance from one dataset  $\mathcal{X}$  to another dataset  $\mathcal{Y}$  is given by  $d(\mathcal{X} \rightarrow \mathcal{Y}) := \sup_{\mathbf{x} \in \mathcal{X}} d(\mathbf{x}, \mathcal{Y}) = \sup_{\mathbf{x} \in \mathcal{X}} \inf_{\mathbf{y} \in \mathcal{Y}} d(\mathbf{x}, \mathbf{y})$ . The *Hausdorff distance* between two datasets  $\mathcal{X}$  and  $\mathcal{Y}$  is defined as

$$d_H(\mathcal{X}, \mathcal{Y}) := \max \{d(\mathcal{X} \rightarrow \mathcal{Y}), d(\mathcal{Y} \rightarrow \mathcal{X})\}.$$

For  $\eta > 0$ , the  $\eta$ -ball of  $\mathbf{x}$  is defined as  $\mathcal{B}_\eta(\mathbf{x}) := \{\mathbf{z} : d(\mathbf{x}, \mathbf{z}) \leq \eta\}$ . The *the  $\eta$ -fattening* of a dataset  $\mathcal{Y}$  is defined as

$$\mathcal{B}_\eta(\mathcal{Y}) := \bigcup_{\mathbf{y} \in \mathcal{Y}} \mathcal{B}_\eta(\mathbf{y}).$$

We say  $\mathcal{Y}$  is a *finite covering* of  $\mathcal{X}$  with radius  $\eta$ , or  $\mathcal{X}$  is *finitely covered* by  $\mathcal{Y}$  with radius  $\eta$ , if  $\mathcal{Y}$  is a finite set and for all  $\mathbf{x} \in \mathcal{X}$ , there exists  $\mathbf{y} \in \mathcal{Y}$  such that  $d(\mathbf{x}, \mathbf{y}) \leq \eta$ , i.e.,  $\mathcal{X} \subseteq \mathcal{B}_\eta(\mathcal{Y})$ . Obviously,  $\mathcal{X}$  is an  $\eta$ -finite covering of itself for any  $\eta > 0$ .

*Remark 3.1.* (1) If  $d(\mathcal{X} \rightarrow \mathcal{Y}) = \eta$ , then  $\mathcal{Y}$  is an  $\eta$ -finite covering of  $\mathcal{X}$ . If  $d_H(\mathcal{X}, \mathcal{Y}) = \eta$ , then  $\mathcal{Y}$  is an  $\eta$ -finite covering of  $\mathcal{X}$ , and  $\mathcal{X}$  is also an  $\eta$ -finite covering of  $\mathcal{Y}$ ;

(2) Any synthetic dataset obtained by coreset and DC methods is a finite covering for some  $\eta > 0$ .

### 4 Minimal Finite Covering (MFC)

In this section, we will connect coreset and DC methods using a unified formulation by posing these dataset compression methods as instances of minimal finite covering (MFC) methods.

Given a dataset  $\mathcal{T} = \{\mathbf{x}_i\}_{i=1}^N \subseteq \mathbb{R}^n$ , the trivial 0-finite covering is the dataset itself, and a trivial  $\infty$ -finite covering can be an arbitrary data. Similarly, there always exists a finite covering of  $\mathcal{T}$  with arbitrary size. Hence the problem of interest is to find the finite covering with minimum radius ( $\eta$ ) or size ( $k$ ).

**Definition 4.1.** For a finite set  $\mathcal{S} \subseteq \mathbb{R}^n$ .

(1) We say  $\mathcal{S}^*$  is an  $\eta$ -Minimal Finite Covering ( $\eta$ -MFC) of  $\mathcal{T}$ , if  $\mathcal{S}^*$  is a finite covering of  $\mathcal{T}$  with fixed radius  $\eta$  and minimum size, i.e.,  $\mathcal{S}$  is one of the minimizers of problem

$$\min_{\mathcal{S}} \{k : d(\mathcal{T} \rightarrow \mathcal{S}) = \eta, |\mathcal{S}| = k\};$$

(2) We say  $\mathcal{S}^*$  is a *k-Minimal Finite Covering (k-MFC)* of  $\mathcal{T}$ , if  $\mathcal{S}^*$  is a finite covering of  $\mathcal{T}$  with fixed size  $k$  and minimum radius, i.e.,  $\mathcal{S}$  is one of the minimizers of problem

$$\min_{\mathcal{S}} \{\eta : d(\mathcal{T} \rightarrow \mathcal{S}) = \eta, |\mathcal{S}| = k\}.$$

*Remark 4.2.* (1) For any  $\eta$  and  $k$ , the  $\eta$ -MFC and  $k$ -MFC always exist, but they are not unique;

(2) We can replace the equality “=” in Definition 4.1 by inequality “ $\leq$ ”. Indeed, any finite covering of  $\mathcal{T}$  with radius  $\leq \eta$  is also a finite covering with radius  $\eta$ . Similarly, any finite covering of  $\mathcal{T}$  with size  $\leq k$  is also a finite covering with size  $k$  by taking repeated points.

Definition 4.1 gives a natural definition of MFC where the term “minimal” is defined with respect to either radius  $\eta$  or size  $k$  of the finite dataset. The following proposition shows that we can also define the MFC using Hausdorff distance. We only take  $\eta$ -MFC as example, the case of  $k$ -MFC can be similarly derived.

**Proposition 4.3.** *The following statements are equivalent:*

- (1)  $\mathcal{S}^*$  is an  $\eta$ -MFC of  $\mathcal{T}$ ;
- (2)  $\mathcal{S}^* \in \arg \min_{\mathcal{S}} \{k : d_H(\mathcal{T}, \mathcal{S}) = \eta, |\mathcal{S}| = k\}$ .

Proof for this proposition is outlined in Appendix A.1.

Notice that, if we assume  $\mathcal{S}$  is a subset of  $\mathcal{T}$ , i.e., a *coreset* of  $\mathcal{T}$ , then the distance from  $\mathcal{S}$  to  $\mathcal{T}$  is exactly 0. In this case, the Hausdorff distance between  $\mathcal{T}$  and  $\mathcal{S}$  reduces to the distance from  $\mathcal{T}$  to  $\mathcal{S}$ , i.e.,  $d_H(\mathcal{T}, \mathcal{S}) = d(\mathcal{T} \rightarrow \mathcal{S})$ , and Proposition 4.3 becomes trivial. The corresponding MFC is called a *minimal coreset (MCS)* of  $\mathcal{T}$ . Any subset of  $\mathcal{T}$  can be described using a binary vector  $\mathbf{s} \in [0, 1]^N$ , where  $s_i = 1$  means  $\mathbf{x}_i \in \mathcal{S}$  otherwise  $\mathbf{x}_i \notin \mathcal{S}$ . In the next theorem, we provide a tractable optimization formulation for MCS.

**Theorem 4.4.** *For a given dataset  $\mathcal{T} = \{\mathbf{x}_i\}_{i=1}^N$ , define the adjacency matrix of  $\mathcal{T}$  w.r.t. radius  $\eta$  as*

$$\mathbf{A}(\eta) := [a_{ij}(\eta)], \quad a_{ij}(\eta) = \begin{cases} 1, & \text{if } d(\mathbf{x}_i, \mathbf{x}_j) \leq \eta; \\ 0, & \text{otherwise.} \end{cases}$$

(1) *The  $\eta$ -MCS of  $\mathcal{T}$  is one of the minimizers of*

$$\min_{\mathbf{s} \in \{0,1\}^N} \{\|\mathbf{s}\|_1 : \mathbf{A}(\eta) \cdot \mathbf{s} \geq \mathbf{1}\}; \quad (\eta\text{-MCS})$$

(2) *The  $k$ -MCS of  $\mathcal{T}$  is one of the minimizers of*

$$\min_{\eta, \mathbf{s} \in \{0,1\}^N} \{\eta : \mathbf{A}(\eta) \cdot \mathbf{s} \geq \mathbf{1}, \|\mathbf{s}\|_1 = k\}. \quad (k\text{-MCS})$$

The proof for this theorem is outlined in Appendix A.2.

*Remark 4.5.* (1) If we adapt the terminology from DC literature, then MFC can be considered as a DC method, and MCS as a coreset selection method;

(2) Finding the  $k$ -MCS of a given dataset is exactly the *K-center* approach (Sener and Savarese, 2018) for coreset selection. In particular, the case of  $k = 1$  is well-known as the *smallest bounding sphere* problem (Elzinga and Hearn, 1972), or the *minimal enclosing ball* problem (Kumar et al., 2004). The *smallest circle* problem in the plane is an example of a *facility location problem* (Fallah et al., 2009). Both the smallest circle problem in the plane, and the smallest bounding sphere problem in any higher-dimensional space of bounded dimension are solvable in worst-case linear time (Megiddo, 1983; Dyer, 1986). However, the K-center problem is NP-hard (Cook et al., 1998).

As we see, determining an  $\eta$ -MCS is equivalent to solving a *mixed integer linear programming (MILP)* problem, while finding a  $k$ -MCS involves addressing a *mixed integer quadratically constrained programming (MIQCP)* problem. Since solving a general MILP is already NP-hard, finding a  $k$ -MCS is much more challenging than finding an  $\eta$ -MCS. Fortunately, we are able to approach the solution of ( $k$ -MCS) by iteratively solving ( $\eta$ -MCS), as shown in Algorithm 1. Indeed, if we fix the radius  $\eta$  in ( $k$ -MCS), then it reduces to a feasibility problem with mixed linear constraints, which gives us an answer whether there exists a valid MCS with radius  $\eta$  and size  $k$ . If the answer is yes, this means we can further decrease the radius and re-check the new feasibility. Otherwise, the radius should be increased until an approximated MCS is found within a specified tolerance precision.

---

**Algorithm 1**  $k$ -MCS

---

**Input:** dataset  $\mathcal{T}$ , size  $k$   
Initialize  $\eta_l \leftarrow 0$ ,  $\eta_u \leftarrow R$ ,  $r \leftarrow \eta_u - \eta_l$ ,  $\delta \leftarrow 10^{-5}$   
**repeat**  
     $\eta_{new} \leftarrow (\eta_l + \eta_u)/2$   
     $v \leftarrow$  feasibility of ( $k$ -MCS) with radius  $\eta_{new}$   
    **if**  $v = \text{TRUE}$  **then**  
         $\eta_l \leftarrow \eta_l$ ,  $\eta_u \leftarrow \eta_{new}$   
    **else**  
         $\eta_l \leftarrow \eta_{new}$ ,  $\eta_u \leftarrow \eta_u$   
    **end if**  
     $r \leftarrow \eta_u - \eta_l$   
**until**  $r \leq \delta$   
**Output:** MCS with given size  $k$  and minimum radius  $\eta_u$

---

## 5 Adversarial Training over $\eta$ -MCS

In this section, we will apply standard- and adversarial- training over the MCS we obtained in the previous section, resulting in the robustness-aware dataset compression method.

Given a probability measure  $\nu$  and a finite dataset  $\mathcal{T} \subseteq \mathbb{R}^{n+1}$ , we assume each data point  $(\mathbf{x}, y) \in \mathcal{T}$  is i.i.d. sampled from  $\nu$ . Each finite sampling  $\mathcal{T}$  defines an empirical distribution  $\hat{\nu}_{\mathcal{T}} = \frac{1}{|\mathcal{T}|} \sum_{(\mathbf{x}, y) \in \mathcal{T}} \delta_{(\mathbf{x}, y)}$ , where  $\delta_{(\mathbf{x}, y)}$  is the Dirac measure over point  $(\mathbf{x}, y)$ . For a loss function  $l : \mathbb{R}^2 \rightarrow \mathbb{R}_+$ , the standard training aims to learn a model parameterized by  $\theta$  that minimizes the standard loss:

$$L^{std}(\theta) = \mathbb{E}_{(\mathbf{x}, y) \sim \nu} [l(f_{\theta}(\mathbf{x}), y)],$$

with its empirical estimation

$$\hat{L}^{std}(\theta, \mathcal{T}) = \mathbb{E}_{(\mathbf{x}, y) \sim \hat{\nu}_{\mathcal{T}}} [l(f_{\theta}(\mathbf{x}), y)].$$

On the other hand, adversarial training aims to learn a model that minimizes the adversarial loss w.r.t. some perturbation  $\varepsilon > 0$ :

$$L_{\varepsilon}^{adv}(\theta) = \mathbb{E}_{(\mathbf{x}, y) \sim \nu} \left[ \max_{\|\delta\| \leq \varepsilon} l(f_{\theta}(\mathbf{x} + \delta), y) \right], \quad (1)$$

with its empirical estimation

$$\hat{L}_{\varepsilon}^{adv}(\theta, \mathcal{T}) = \mathbb{E}_{(\mathbf{x}, y) \sim \hat{\nu}_{\mathcal{T}}} \left[ \max_{\|\delta\| \leq \varepsilon} l(f_{\theta}(\mathbf{x} + \delta), y) \right]. \quad (2)$$

In the following discussion, we will focus on classification task, i.e.,  $y \in \{1, \dots, K\}$ . For a probability measure  $\nu$  and a fixed label  $i$ , we denote by  $\mathcal{T}_i \subseteq \mathbb{R}^n$  an i.i.d sampling from the conditional probability measure  $\nu(\cdot | y = i)$ . We assume that  $\mathcal{T}_i \cap \mathcal{T}_j = \emptyset$  for all  $i \neq j$ , since one single point cannot share two different labels. In adversarial training, we are also searching around the ball of radius  $\varepsilon$  for each point, which is exactly the  $\varepsilon$ -fattening of dataset  $\mathcal{T}$ . Therefore, we also need to make sure that the two fattening balls of different labels do not overlap.

**Definition 5.1.** We say that  $\{\mathcal{T}_i\}$  satisfy the *Running Isolation Property (RIP)* if for all  $i \neq j$ , the sets  $\mathcal{T}_i$  and  $\mathcal{T}_j$  do not overlap, i.e.,  $\mathcal{T}_i \cap \mathcal{T}_j = \emptyset$ .

**Assumption 5.2.** In standard training, we assume  $\{\mathcal{T}_i\}$  satisfies RIP. In adversarial training, we assume  $\varepsilon$  is such that  $\{\mathcal{B}_{\varepsilon}(\mathcal{T}_i)\}$  satisfies RIP. In this case, we also say that  $\mathcal{T}$  is  $\varepsilon$ -separated borrowing the terminology in (Yang et al., 2020; Li et al., 2022).

*Remark 5.3.* Assumption 5.2 is easily satisfied by setting  $\varepsilon < \min_{j \neq k} d(\mathcal{T}_j, \mathcal{T}_k)/2$ .

While performing adversarial training over MCS, we can simply use the classical definition of adversarial loss in Equation (1) and Equation (2), i.e., set equal weights to each individual Dirac measure in the empirical distribution  $\hat{\nu}_{\mathcal{T}}$ . However, by doing this, we are unable to derive any provable

relation between the empirical adversarial loss over the compressed dataset and the original one. Fortunately, for MCS, we can define the generalized adversarial loss to provide a provable guarantee compared to the classical loss.

**Definition 5.4.** Let  $\mathcal{T} = \cup_i \mathcal{T}_i$  be a finite sampling from  $\nu$  where each  $\mathcal{T}_i$  is the conditional sampling from  $\nu(\cdot|y=i)$ . Suppose  $\mathcal{S} = \cup_i \mathcal{S}_i$  is an  $\eta$ -MCS of  $\mathcal{T}$  such that  $\{\mathcal{B}_{\varepsilon+\eta}(\mathcal{S}_i)\}$  satisfies RIP,

(1) The *generalized empirical distribution* over  $\mathcal{S}$  is defined:

$$\hat{\mu}_{\mathcal{S}} = \frac{1}{|\mathcal{T}|} \sum_{(\mathbf{x},y) \in \mathcal{S}} q_{(\mathbf{x},y)} \delta_{(\mathbf{x},y)},$$

where  $q_{(\mathbf{x},y)}$  is the number of points in  $\mathcal{T}$  that belongs to the ball  $\mathcal{B}_{\eta}(\mathbf{x})$ ;

(2) The *generalized adversarial loss* over  $\mathcal{S}$  is defined as

$$\hat{G}_{\varepsilon+\eta}^{adv}(\theta, \mathcal{S}) := \mathbb{E}_{(\mathbf{x},y) \sim \hat{\mu}_{\mathcal{S}}} \left[ \max_{\|\delta\| \leq \varepsilon+\eta} l(f_{\theta}(\mathbf{x} + \delta), y) \right].$$

By adding non-trivial weights to the classical adversarial loss, we are able to derive a provable guarantee of the generalized adversarial loss.

**Theorem 5.5.** Let  $\mathcal{T}$  and  $\mathcal{S}$  be as defined in Definition 5.4. Then  $\hat{L}_{\varepsilon}^{adv}(\theta, \mathcal{T}) \leq \hat{G}_{\varepsilon+\eta}^{adv}(\theta, \mathcal{S})$ .

Proof for this theorem is outlined in Appendix A.3.

From Theorem 5.5, we are glad to see that, minimizing the generalized adversarial loss over MCS provides a valid upper bound of minimizing the classical adversarial loss over the original dataset. Note that if  $\eta = 0$ , the generalized adversarial loss reduces to the classical one.

**Corollary 5.6.** Let  $\mathcal{T}$  and  $\mathcal{S}$  be as defined in Definition 5.4, then the robust model obtained by minimizing the generalized adversarial loss  $\hat{G}_{\varepsilon+\eta}^{adv}(\theta, \mathcal{S})$  is robust over the original dataset  $\mathcal{T}$  w.r.t. radius  $\varepsilon$ .

## 6 Revisiting the Trade-off between Accuracy and Robustness

Before going into the experimental results, we discuss some well-known results of accuracy and robustness of models, and how they behave for different datasets. We first give the formal definition of test accuracy and robust accuracy, which are the core concepts throughout the following discussion.

**Definition 6.1.** Given a probability measure  $\nu$ , an i.i.d. sampling  $\mathcal{T}$  from  $\nu$  with its associated empirical measure  $\hat{\nu}_{\mathcal{T}}$ , and a hypothesis space  $\mathcal{H}$ . For  $\theta \in \mathcal{H}$ ,

(1) The *test accuracy* of  $\theta$  is defined as

$$TA(\theta) := \Pr_{(\mathbf{x},y) \sim \nu} [f_{\theta}(\mathbf{x}) = y],$$

with its empirical version

$$\widehat{TA}(\theta, \mathcal{T}) := \Pr_{(\mathbf{x},y) \sim \hat{\nu}_{\mathcal{T}}} [f_{\theta}(\mathbf{x}) = y];$$

(2) The *robust accuracy* of  $\theta$  w.r.t. perturbation  $\varepsilon$  is defined:

$$RA(\varepsilon, \theta) := \Pr_{(\mathbf{x},y) \sim \nu} [f_{\theta}(\mathbf{x} + \delta) = y, \forall \|\delta\| \leq \varepsilon],$$

with its empirical version

$$\widehat{RA}(\varepsilon, \theta, \mathcal{T}) := \Pr_{(\mathbf{x},y) \sim \hat{\nu}_{\mathcal{T}}} [f_{\theta}(\mathbf{x} + \delta) = y, \forall \|\delta\| \leq \varepsilon].$$

It is well known that there is a trade-off between test accuracy and robustness (Tsipras et al., 2019; Zhang et al., 2019b; Yang et al., 2020; Raghunathan et al., 2020) for deep neural networks. This is to say that, if the test accuracy of a model  $TA(\theta)$  is high (which can be achieved by standard training), then its robust accuracy  $RA(\varepsilon, \theta)$  is usually low, i.e., any classifier that is very accurate will necessarily be non-robust. Identically, if the robust accuracy of a model  $RA(\varepsilon, \theta)$  is high (which can be achieved by adversarial training), then its test accuracy  $TA(\theta)$  is usually low. In one sentence:



*It is usually difficult for a classifier to be both accurate and robust.*

The accuracy-robustness trade-off we described above is about the performance of classifiers in  $\mathcal{H}$  over a fixed probability measure  $\nu$  or  $\hat{\nu}_{\mathcal{T}}$ . For every dataset  $\mathcal{T}$ , we define the *standard classifier* as  $\theta_{\mathcal{T}}^{std} = \arg \min_{\theta \in \mathcal{H}} \widehat{TA}(\theta, \mathcal{T})$ , and the *robust classifier* as  $\theta_{\varepsilon, \mathcal{T}}^{adv} = \arg \min_{\theta \in \mathcal{H}} \widehat{RA}(\varepsilon, \theta, \mathcal{T})$ . If we focus on the optimal classifiers  $\theta_{\mathcal{T}}^{std}, \theta_{\varepsilon, \mathcal{T}}^{adv}$  depending only on  $\mathcal{T}$ , then we can also discuss about the accuracy and robustness of different datasets  $\mathcal{T}$ .

**Definition 6.2.** Given a finite dataset  $\mathcal{T}$ .

- (1) The *test score* of  $\mathcal{T}$  is defined as the test accuracy of the standard classifier  $\theta_{\mathcal{T}}^{std}$ , i.e.,  $TS(\mathcal{T}) = TA(\theta_{\mathcal{T}}^{std})$ ;
- (2) The *robust score* of  $\mathcal{T}$  w.r.t. perturbation  $\varepsilon$  is defined as the robust accuracy of the robust classifier  $\theta_{\varepsilon, \mathcal{T}}^{adv}$ , i.e.,  $RS(\varepsilon, \mathcal{T}) = RA(\varepsilon, \theta_{\varepsilon, \mathcal{T}}^{adv})$ .

In the current DC literature, most of the methods are proposed to maximize the test score of dataset  $\mathcal{T}$ , resulting in solving the optimization problem:  $\max_{\mathcal{T}} TS(\mathcal{T})$ . This has shown excellent performance even for extreme dataset compression, despite the expensive computation and heavy memory burden (Cui et al., 2022). Take the CIFAR10 dataset (Krizhevsky et al., 2009), for example, we are able to achieve 71.6% test accuracy over a synthetic dataset with only 50 images per class v.s. 84.8% over the original dataset with 50000 images in total, according to (Cazenavette et al., 2022).

However, to the best of the authors' knowledge, there are no existing works concerned about the robustness of models trained with these synthetic, compressed, datasets. In this work, we re-observed the accuracy-robustness trade-off for compressed datasets: if the test score of a dataset  $TS(\mathcal{T})$  is high (which can be achieved by DC methods), then their robust score  $RS(\varepsilon, \mathcal{T})$  is usually low, which means adversarial training over  $\mathcal{T}$  is not effective. We therefore propose the following conjecture:

*It is usually difficult for a compressed dataset to be both accurate and robust.*

Similar to Tsipras et al. (2019), we give an explicit example to illustrate the above conjecture.

**Example 6.3.** (*Robustness-accuracy trade-off for compressed dataset*). Consider a binary classification task for data  $(\mathbf{x}, y) \in \mathbb{R}^{n+1} \times \{\pm 1\}$  sampled from distribution  $\nu(p)$  defined as follows:

$$\begin{aligned}
 y &\sim \mathcal{U}(\{\pm 1\}), \\
 x_1 &= \begin{cases} +y, & \text{w.p. } p, \\ -y, & \text{w.p. } 1 - p, \end{cases} \\
 x_2, \dots, x_{n+1} &\stackrel{i.i.d.}{\sim} \mathcal{U}([(y-1)/2, (y+1)/2]).
 \end{aligned}$$

Let the hypothesis space  $\mathcal{H}$  be the space of linear classifiers  $\text{sign}(\mathbf{w}^T \mathbf{x})$ , and consider  $\ell_{\infty}$ -adversarial robustness with perturbation  $\varepsilon = 1$ . Then, for any  $p \in [0.5, 1]$ ,

- (1) Any classifier  $f_a(\mathbf{x}) = \text{sign}(w_2 x_2 + \dots + w_{n+1} x_{n+1})$  with  $w_i > 0$  is perfect, i.e.,  $TA(f) = 100\%$ , but has robust accuracy 0%;
- (2) The most robust classifier is  $f_r(\mathbf{x}) = \text{sign}(x_1)$ , with test and robust accuracy both equal to  $p$ .

Example 6.3 indicates that, on the one hand, we always have perfect but non-robust classifiers  $f_a$  for any distribution  $\nu(p)$ . On the other hand, the robust accuracy of any classifier cannot be higher than  $p$ . In this case, DC methods can easily achieve the best test performance. However, the compressed datasets might not follow the original data distribution. For the synthetic datasets sampled from distribution  $\nu(p)$  with  $p \approx 0.5$ , it is impossible to improve the robust accuracy of the classifiers to a satisfactory level.

## 7 Experiments

In this section, we provide additional evidence supporting the trade-off between robustness and accuracy for compressed dataset, as previously discussed. Our experiments are conducted on a toy dataset with four classes: [I,C,M,L], and two benchmark datasets (MNIST and CIFAR10). We explore three dataset compression methods:

Table 1: Comparison of test and robust accuracy of models trained over DIKU dataset. The coresets we consider are **RAW** and **MCS- $\eta$**  of fixed radius  $\eta = 0.05$  and minimum size  $k = 75$ . The perturbation of  $\ell_\infty$ -adversarial robustness is 0.05.

CORESET	TRAIN	TEST ACC.	$\ell_\infty$ ACC.
RAW	STD	100	88.20
	$\ell_\infty$ -ADV	100	<b>91.65</b>
MCS- $\eta$	STD	100	89.09
	$\ell_\infty$ -ADV	99.89	90.53
	GEN. $\ell_\infty$ -ADV	100	<b>95.43</b>

- **RAW**: original full dataset;
- **RAND- $k$** : random coreset selection of size  $k$ ;
- **DM- $k$** : distribution matching of size  $k$ ;
- **MCS- $\varepsilon$** : MCS of radius  $\varepsilon$  by solving problem ( $\eta$ -MCS);
- **MCS- $k$** : MCS of size  $k$  using Algorithm 1.

We mainly consider DM from Zhao and Bilen (2023) as the baseline DC method due to the considerable computational costs associated with obtaining the compressed datasets from other DC methods involving bi-level optimizations; particularly when scaling up the size, such as with  $k = 500$ . We choose the computationally cheaper DM method, as the baseline which also shows competitive performance compared to other DC methods (Cui et al., 2022). For each compressed dataset, we consider a multilayer perceptron (MLP) for the toy- and MNIST- datasets, and convolutional neural networks (ConvNet) for CIFAR10 dataset. Specifically, the MLP architecture consists of two hidden layers, each comprising 128 neurons. The ConvNet architecture includes 3 blocks, each containing 128 filters of size  $3 \times 3$ , followed by instance norm (Ulyanov et al., 2016), ReLU activation and average pooling layers. We perform generalized adversarial training over the MCS, and classical adversarial training over other compressed dataset.

For all datasets, we focus on MCS w.r.t.  $\ell_2$ -norm, and perform adversarial training over them for both  $\ell_\infty$ - and  $\ell_2$ - norms. This is because MNIST and CIFAR10 data are distributed very closely to the boundary of  $\ell_\infty$ -balls, resulting in similar  $\ell_\infty$ -distances between data points within the same class. All the MCS are obtained using the existing MILP solver in GUROBI by solving ( $\eta$ -MCS). Experimental results for MCS with respect to  $\ell_\infty$ -norm are presented in Appendix B.4. We use PGD- $\ell_\infty$  and PGD- $\ell_2$  attack to perform adversarial training and compute the robust accuracy. Following the common setting in the robustness literature (Croce et al., 2020), we set the adversarial perturbation to  $\varepsilon_\infty = 0.1$  for MNIST dataset and  $\varepsilon_\infty = 8/255$  for CIFAR10 dataset, for  $\ell_\infty$ -norm. For  $\ell_2$ -norm, in order to keep the volume of  $\ell_\infty$ -ball and  $\ell_2$ -ball be similar, we set  $\varepsilon_2 = \sqrt{\frac{2n}{\pi e}} \varepsilon_\infty$ , where  $n$  is the (flattened) dimension of input images. All the experiments are run with 5 repeats using an NVIDIA A100 40GB GPU. Source code will be made available at <https://github.com/saintslab/pytoch>.

## 7.1 “DIKU”<sup>1</sup> dataset

We first construct a two-dimensional toy dataset with four labels: “D”, “I”, “K” and “U” and consisting of 898 points. By computing the minimum distance of subset with different labels, we get that this dataset is 0.2-separated. Therefore we consider  $\ell_\infty$ -adversarial robustness with perturbation  $\varepsilon = 0.05$ , and the maximum radius of finite covering that satisfies Theorem 5.5 is  $\eta = 0.05$ . By solving problem ( $\eta$ -MCS), we obtain a 0.05-MCS with minimum size  $k = 75$ . Figure 4 in Appendix B.1 is the visualization of “DIKU” dataset and its  $\eta$ -MCS. We first apply standard training and adversarial

<sup>1</sup>The Danish abbreviation of Dept. of Computer Science at University of Copenhagen ends up being DIKU



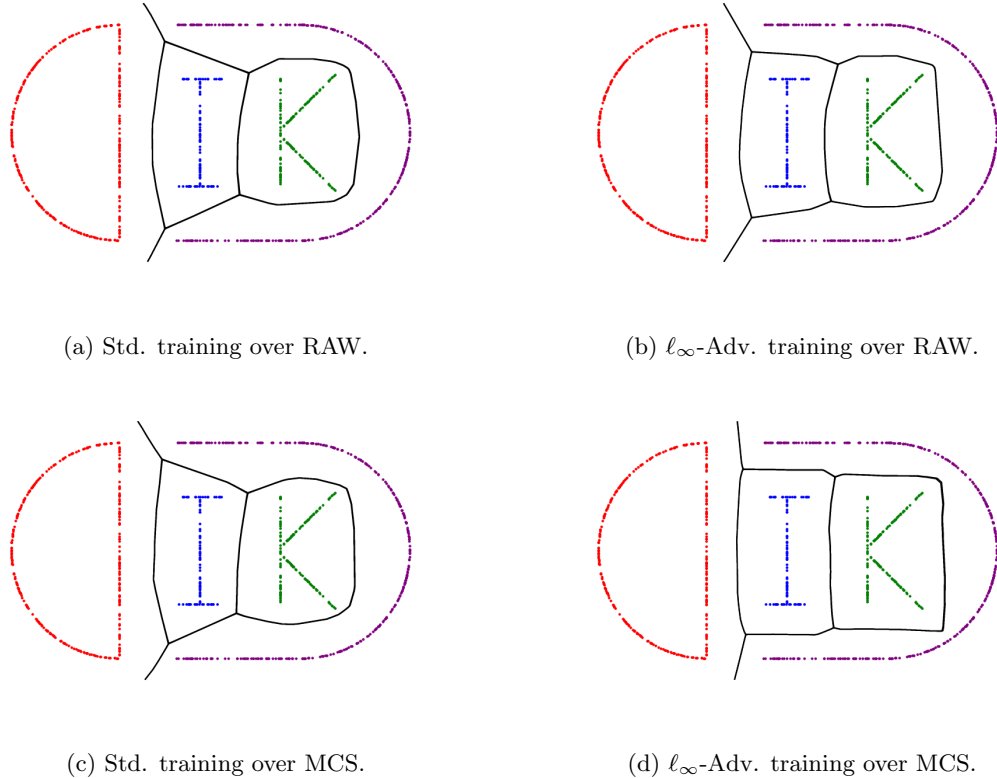


Figure 1: Visualization of the DIKU toy dataset and decision boundaries of models trained using various coresets. Figures in the first and second rows are results for standard training and  $\ell_\infty$ -adversarial training respectively. Figures in the first and second columns are results for coresets **RAW** and **MCS** respectively. The black solid lines are the decision boundaries of each model. The decision boundary between "K" and "U" (the right vertical line) clearly exemplifies the influence of robustness-aware training, as the margin between the classes is the largest for  $\ell_\infty$ -adversarial training in (b) and (d) compared to the other two settings.

training (with perturbation  $\varepsilon$ ) over the full dataset as a baseline. For  $\eta$ -MCS, we use perturbation  $\varepsilon + \eta$  instead of  $\varepsilon$  for (generalized) adversarial training.

Table 1 shows the downstream performance of models trained over the original dataset and compressed dataset. We see that adversarial training is essential to improve robustness, and there is no remarkable discrepancy between the test accuracy of standardly trained models (98.97% v.s. 97.66%) and the robust accuracy of adversarially trained models (78.85% v.s. 75.82%). These experimental results give strong evidence to the statement in Theorem 5.5. Figure 1 shows the visualization of the decision boundaries of models trained with the original- and compressed datasets. Figure 5 in Appendix B.2 additionally shows the visual comparison of classical and generalized adversarial training over MCS of DIKU dataset.

## 7.2 MNIST and CIFAR10 dataset

For convenience of comparison, we consider  $k$ -MCS for both MNIST and CIFAR10 dataset with  $k = [50, 100, 200, 300, 400, 500]$ . However, for these considered sizes, their corresponding radius  $\eta$  is quite large and the  $(\varepsilon + \eta)$ -fattening of the MCS does not satisfy RIP. Thus Theorem 5.5 is not applicable here anymore. Nevertheless, we can still perform generalized adversarial training over MCS, with perturbation  $\varepsilon$  instead of  $\varepsilon + \eta$ . We will see later that it actually shows excellent empirical downstream performance. Table 3 in Appendix B.3 shows the hyperparameters for standard and adversarial training for MNIST and CIFAR10 dataset.

Figure 2 shows the test,  $\ell_\infty$ - and  $\ell_2$ - robust accuracy of models obtained by standard,  $\ell_\infty$ - and  $\ell_2$ -

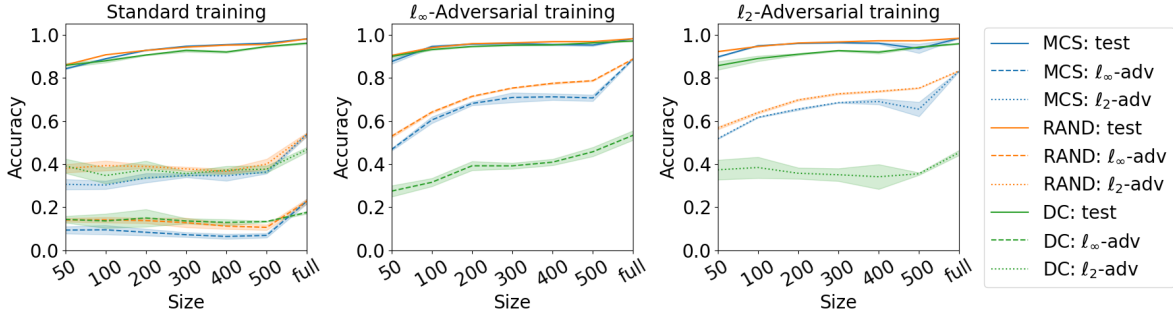


Figure 2: Performance of standard and robust models trained with different compressed datasets from MNIST. The figures from left to right are standard training,  $\ell_\infty$ -adversarial training and  $\ell_2$ -adversarial training. The blue, orange and green lines stand for **MCS**, **RAND**, and **DM** respectively. The solid, dashed and dotted lines stand for test,  $\ell_\infty$  and  $\ell_2$  robust accuracy respectively. In the horizontal axis, “full” means the original dataset for **MCS** and **RAND**, and  $k = 5000$  for **DM**.

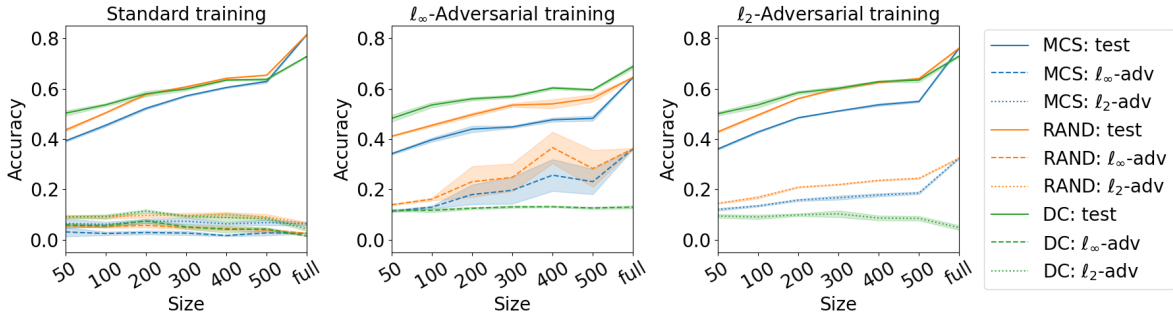


Figure 3: Performance of standard and robust models trained over different compressed dataset from CIFAR10. The figures from left to right are standard training,  $\ell_\infty$ -adversarial training and  $\ell_2$ -adversarial training. The blue, orange and green lines stand for **MCS**, **RAND**, and **DM** respectively. The solid, dashed and dotted lines stand for test,  $\ell_\infty$  and  $\ell_2$  robust accuracy respectively. In the horizontal axis, “full” means the original dataset for **MCS** and **RAND**, and  $k = 4000$  for **DM**.

adversarial training over the original MNIST and compressed dataset. Notice that for **RAND- $k$**  and **MCS- $k$** , the coresets becomes exactly the original dataset if  $k = N$ . However, even though  $k = N$ , **DM- $k$**  is still different from the original dataset. We compute **DM- $k$**  with  $k = 5000$  for MNIST dataset. We see that, when applying standard training, all models show similar performance in terms of test accuracy and robust accuracy. However, adversarial training over **DM- $k$**  does not seem to be more effective, while **RAND- $k$**  and **MCS- $k$**  have large improvement in robustness. Even if the size of **DM** increases to  $k = 5000$ , the robust accuracy after adversarial training is still *much* lower than when using the original dataset. This behavior coincides with the conjecture we propose in Section 6: DC methods breaks the distribution of the original data.

Figure 3 shows exactly the same behavior for CIFAR10 dataset. Due to memory issue, we only have access to **DM- $k$**  with  $k = 4000$ . As the size of compressed dataset increases, the robust accuracy of both **MCS** and **RAND** are both increasing. However, the robustness of **DM** does not seem to improve. Especially if we increase the size  $k$  of **DM** to 4000, the test accuracy of  $\ell_\infty$ -robustly trained model slightly outperforms the original CIFAR10 data (68.86% v.s. 64.59%), whereas the robust score of the former is *much* smaller than the latter (12.98% v.s. 36.21%), which is actually at the same level as  $k = 50$ .

Table 2 provides an overview of all the numerical results evaluated over different models and different datasets. All the results are computed by the mean of 5 repeats and their standard deviation. Surprisingly, the poor behavior of **DM** is expected, but **RAND** performs even better than **MCS** in most cases, both for test and robust accuracy. This makes sense because RIP condition does not hold either for MNIST or CIFAR10, whereas the random coreset might capture the distribution of the original data better.

Table 2: Downstream performance of models trained over original and compressed dataset of MNIST and CIFAR10. The considered coresets are **RAW**, **MCS- $k$** , **RAND- $k$**  with  $k = 500$ , and **DM- $k$**  with  $k = 500$ . To compare **DM** with **RAW**, we set the size of **DM** to be 5000 and 4000 for MNIST and CIFAR10 respectively. The  $\ell_\infty$  perturbation radius of MNIST and CIFAR10 is 0.1 and 8/255 respectively. The  $\ell_2$  perturbation radius of MNIST and CIFAR10 is 1.36 and 0.84.

DATASET	CORESET	TEST SCORE	$\ell_\infty$ -SCORE	$\ell_2$ -SCORE
MNIST	RAW	98.08±0.06	88.75±0.23	83.29±0.19
	MCS-500	<b>96.10</b> ±0.15	70.69±1.44	65.46±3.31
	RAND-500	95.47±0.02	<b>78.69</b> ±0.28	<b>75.23</b> ±0.20
	DM-500	94.51±0.28	45.72±2.11	35.50±0.57
	DM-5000	96.04±0.40	53.37±2.19	45.34±1.19
CIFAR10	RAW	81.64±0.15	36.21±0.23	32.50±0.27
	MCS-500	62.89±0.54	23.09±5.01	18.59±0.49
	RAND-500	<b>65.42</b> ±0.18	<b>28.30</b> ±7.31	<b>24.42</b> ±0.27
	DM-500	63.76±0.38	12.61±0.46	8.50±0.89
	DM-4000	72.91±0.36	12.98±0.56	4.81±0.90

## 8 Conclusion and Future Works

In this paper, we stress the accuracy-robustness trade-off in terms of compressed datasets, which is rarely discussed in the robustness and DC communities. We claim that improving both the test score and robust score of a dataset is difficult, because DC methods force the dataset to *only* maximize the test performance and breaks the data distribution. We construct a probabilistic example and show several numerical experiments to support our arguments.

Moreover, in order to perform adversarial training with compressed datasets with provable guarantee, we propose MCS and generalized adversarial loss over MCS. We proved that the generalized adversarial loss over MCS provides a valid upper bound of the classical adversarial loss over the original dataset. This means if the data satisfies RIP condition, i.e.,  $(\varepsilon + \eta)$ -separated, then there exists a robust classifier over MCS w.r.t. radius  $\varepsilon + \eta$  which is also robust over the original dataset w.r.t. radius  $\varepsilon$ . Even though this condition does not hold for MNIST and CIFAR10, there is empirical improvement compared to the DC method.

Finally, we propose an MILP formulation to obtain MCS with fixed radius or size. The advantage of MCS is three folds: firstly, it is a one-time computation, which means the MCS can be applied to any models for any tasks; secondly, the MCS can be adapted to different distance metrics; lastly, the size of MILP only depends on the number of data, not on the dimension of data.

There are many interesting future works regarding DC and robustness. For example, we showed that compressed datasets obtained by DC methods have poor robustness scores. Investigations into enabling robust DC methods will be of interest. Further proving the accuracy-robustness trade-off in a more general setting will also be interesting.

## Broader Impact

This paper presents work whose goal is to advance the field of Machine Learning. However, the work here could raise awareness about the trade-off between performance, efficiency, and robustness, of a small class of ML methods. There are many potential societal consequences of our work, none which we feel must be further highlighted here.

## Acknowledgements

The authors acknowledge funding received under European Union’s Horizon Europe Research and Innovation programme under grant agreements No. 101070284 and No. 101070408. The authors thank Julian E Schön for useful discussions during the early development of the work.

## References

- I. M. Alabdulmohsin, B. Neyshabur, and X. Zhai. Revisiting neural scaling laws in language and vision. *Advances in Neural Information Processing Systems (NeurIPS)*, 35:22300–22312, 2022.
- L. F. W. Anthony, B. Kanding, and R. Selvan. Carbontracker: Tracking and Predicting the Carbon Footprint of Training Deep Learning Models. ICML Workshop on Challenges in Deploying and monitoring Machine Learning Systems, 2020.
- B. R. Bartoldson, B. Kaikhura, and D. Blalock. Compute-efficient deep learning: Algorithmic trends and opportunities. *Journal of Machine Learning Research*, 24:1–77, 2023.
- E. M. Bender, T. Gebru, A. McMillan-Major, and S. Shmitchell. On the dangers of stochastic parrots: Can language models be too big? In *Proceedings of the 2021 ACM conference on fairness, accountability, and transparency (FaCT)*, 2021.
- N. Carlini, F. Tramer, K. D. Dvijotham, L. Rice, M. Sun, and J. Z. Kolter. (certified!!) adversarial robustness for free! In *The Eleventh International Conference on Learning Representations*, 2023.
- G. Cazenavette, T. Wang, A. Torralba, A. A. Efros, and J.-Y. Zhu. Dataset distillation by matching training trajectories. In *Proceedings of the IEEE/CVF Conference on Computer Vision and Pattern Recognition*, 2022.
- K. Chen. On coresets for k-median and k-means clustering in metric and euclidean spaces and their applications. *SIAM Journal on Computing*, 39(3):923–947, 2009. doi: 10.1137/070699007.
- Y. Chen, M. Welling, and A. Smola. Super-samples from kernel herding. In *Proceedings of the Twenty-Sixth Conference on Uncertainty in Artificial Intelligence*, pages 109–116, 2010.
- J. Cohen, E. Rosenfeld, and Z. Kolter. Certified adversarial robustness via randomized smoothing. In K. Chaudhuri and R. Salakhutdinov, editors, *Proceedings of the 36th International Conference on Machine Learning*, volume 97 of *Proceedings of Machine Learning Research*, pages 1310–1320. PMLR, 09–15 Jun 2019.
- W. J. Cook, W. H. Cunningham, W. R. Pulleyblank, and A. Schrijver. *Combinatorial Optimization*. John Wiley & Sons, Inc., USA, 1998. ISBN 047155894X.
- F. Croce, M. Andriushchenko, V. Schwag, E. Debenedetti, N. Flammarion, M. Chiang, P. Mittal, and M. Hein. Robustbench: a standardized adversarial robustness benchmark. *arXiv preprint arXiv:2010.09670*, 2020.
- J. Cui, R. Wang, S. Si, and C.-J. Hsieh. Dc-bench: Dataset condensation benchmark. *arXiv preprint arXiv:2207.09639*, 2022.
- M. E. Dyer. On a multidimensional search technique and its application to the euclidean one-centre problem. *SIAM Journal on Computing*, 15(3):725–738, 1986. doi: 10.1137/0215052.
- D. J. Elzinga and D. W. Hearn. The minimum covering sphere problem. *Management Science*, 19(1): 96–104, 1972. ISSN 00251909, 15265501.
- H. Fallah, A. N. Sadigh, and M. Aslanzadeh. *Covering Problem*, pages 145–176. Physica-Verlag HD, Heidelberg, 2009. ISBN 978-3-7908-2151-2. doi: 10.1007/978-3-7908-2151-2\_7.
- R. Z. Farahani and M. Hekmatfar. *Facility location: concepts, models, algorithms and case studies*. Springer Science & Business Media, 2009.
- C. Finlay and A. M. Oberman. Scaleable input gradient regularization for adversarial robustness. *Machine Learning with Applications*, 3:100017, 2021. ISSN 2666-8270. doi: <https://doi.org/10.1016/j.mlwa.2020.100017>.
- M. Goldblum, L. Fowl, S. Feizi, and T. Goldstein. Adversarially robust distillation. *Proceedings of the AAAI Conference on Artificial Intelligence*, 34(04):3996–4003, Apr. 2020. doi: 10.1609/aaai.v34i04.5816.

- I. Goodfellow, J. Shlens, and C. Szegedy. Explaining and harnessing adversarial examples. In *International Conference on Learning Representations*, 2015.
- S. Goyal, K. Dvijotham, R. Stanforth, R. Bunel, C. Qin, J. Uesato, R. Arandjelovic, T. Mann, and P. Kohli. On the effectiveness of interval bound propagation for training verifiably robust models. *arXiv preprint arXiv:1810.12715*, 2018.
- S. Gui, H. Wang, H. Yang, C. Yu, Z. Wang, and J. Liu. Model compression with adversarial robustness: A unified optimization framework. In *Proceedings of the 33rd Conference on Neural Information Processing Systems*, 2019.
- G. Hinton, O. Vinyals, and J. Dean. Distilling the knowledge in a neural network. *Advances in Neural Information Processing Systems (NeurIPS)*, 2014.
- S. Hooker, N. Moorosi, G. Clark, S. Bengio, and E. Denton. Characterising bias in compressed models. *Arxiv*, 2020.
- L. H. Kaack, P. L. Donti, E. Strubell, G. Kamiya, F. Creutzig, and D. Rolnick. Aligning artificial intelligence with climate change mitigation. *Nature Climate Change*, 2022.
- J. Kaplan, S. McCandlish, T. Henighan, T. B. Brown, B. Chess, R. Child, S. Gray, A. Radford, J. Wu, and D. Amodei. Scaling laws for neural language models. *arXiv preprint arXiv:2001.08361*, 2020.
- A. Krizhevsky, G. Hinton, et al. Learning multiple layers of features from tiny images. 2009.
- P. Kumar, J. S. B. Mitchell, and E. A. Yildirim. Approximate minimum enclosing balls in high dimensions using core-sets. *ACM J. Exp. Algorithmics*, 8:1.1–es, dec 2004. ISSN 1084-6654. doi: 10.1145/996546.996548.
- Y. LeCun, Y. Bengio, and G. Hinton. Deep learning. *nature*, 521(7553):436–444, 2015.
- M. Lecuyer, V. Atlidakis, R. Geambasu, D. Hsu, and S. Jana. Certified robustness to adversarial examples with differential privacy. In *2019 IEEE Symposium on Security and Privacy (SP)*, pages 656–672, 2019. doi: 10.1109/SP.2019.00044.
- B. Li, J. Jin, H. Zhong, J. Hopcroft, and L. Wang. Why robust generalization in deep learning is difficult: Perspective of expressive power. In S. Koyejo, S. Mohamed, A. Agarwal, D. Belgrave, K. Cho, and A. Oh, editors, *Advances in Neural Information Processing Systems*, volume 35, pages 4370–4384. Curran Associates, Inc., 2022.
- A. Madry, A. Makelov, L. Schmidt, D. Tsipras, and A. Vladu. Towards deep learning models resistant to adversarial attacks. In *International Conference on Learning Representations (ICLR)*, 2018.
- N. Megiddo. Linear-time algorithms for linear programming in  $r^3$  and related problems. *SIAM Journal on Computing*, 12(4):759–776, 1983. doi: 10.1137/0212052.
- M. Mirman, T. Gehr, and M. Vechev. Differentiable abstract interpretation for provably robust neural networks. In J. Dy and A. Krause, editors, *Proceedings of the 35th International Conference on Machine Learning*, volume 80 of *Proceedings of Machine Learning Research*, pages 3578–3586. PMLR, 10–15 Jul 2018.
- M. N. Mueller, F. Eckert, M. Fischer, and M. Vechev. Certified training: Small boxes are all you need. In *The Eleventh International Conference on Learning Representations*, 2023.
- A. Raghunathan, J. Steinhardt, and P. Liang. Certified defenses against adversarial examples. *arXiv preprint arXiv:1801.09344*, 2018.
- A. Raghunathan, S. M. Xie, F. Yang, J. Duchi, and P. Liang. Understanding and mitigating the tradeoff between robustness and accuracy. In H. D. III and A. Singh, editors, *Proceedings of the 37th International Conference on Machine Learning*, volume 119 of *Proceedings of Machine Learning Research*, pages 7909–7919. PMLR, 13–18 Jul 2020.
- J. Schmidhuber. Deep learning in neural networks: An overview. *Neural networks*, 61:85–117, 2015.

- R. Selvan, J. Schön, and E. B. Dam. Operating critical machine learning models in resource constrained regimes. In *MICCAI Workshop on Resource-Efficient Medical Image Analysis*. Springer, 2023.
- O. Sener and S. Savarese. Active learning for convolutional neural networks: A core-set approach. In *International Conference on Learning Representations*, 2018.
- S. Stoychev and H. Gunes. The effect of model compression on fairness in facial expression recognition. *Arxiv*, 2022.
- E. Strubell, A. Ganesh, and A. McCallum. Energy and policy considerations for modern deep learning research. In *Proceedings of the AAAI conference on artificial intelligence*, volume 34, pages 13693–13696, 2020.
- F. Tramèr, A. Kurakin, N. Papernot, I. Goodfellow, D. Boneh, and P. McDaniel. Ensemble adversarial training: Attacks and defenses. In *International Conference on Learning Representations*, 2018.
- D. Tsipras, S. Santurkar, L. Engstrom, A. Turner, and A. Madry. Robustness may be at odds with accuracy. In *International Conference on Learning Representations*, 2019.
- D. Ulyanov, A. Vedaldi, and V. Lempitsky. Instance normalization: The missing ingredient for fast stylization. *arXiv preprint arXiv:1607.08022*, 2016.
- K. Wang, B. Zhao, X. Peng, Z. Zhu, S. Yang, S. Wang, G. Huang, H. Bilen, X. Wang, and Y. You. Cafe: Learning to condense dataset by aligning features. In *2022 IEEE/CVF Conference on Computer Vision and Pattern Recognition (CVPR)*, pages 12186–12195, 2022. doi: 10.1109/CVPR52688.2022.01188.
- T. Wang, J.-Y. Zhu, A. Torralba, and A. A. Efros. Dataset distillation. *arXiv preprint arXiv:1811.10959*, 2018.
- D. Wright, C. Igel, G. Samuel, and R. Selvan. Efficiency is not enough: A critical perspective of environmentally sustainable ai. *Arxiv*, 2023.
- Y.-Y. Yang, C. Rashtchian, H. Zhang, R. R. Salakhutdinov, and K. Chaudhuri. A closer look at accuracy vs. robustness. In H. Larochelle, M. Ranzato, R. Hadsell, M. Balcan, and H. Lin, editors, *Advances in Neural Information Processing Systems*, volume 33, pages 8588–8601. Curran Associates, Inc., 2020.
- S. Ye, K. Xu, S. Liu, J.-H. Lambrechts, H. Zhang, A. Zhou, K. Ma, Y. Wang, and X. Lin. Adversarial robustness vs. model compression, or both? In *The IEEE International Conference on Computer Vision (ICCV)*, October 2019.
- H. Zhang, T.-W. Weng, P.-Y. Chen, C.-J. Hsieh, and L. Daniel. Efficient neural network robustness certification with general activation functions. In *Advances in Neural Information Processing Systems (NuerIPS)*, dec 2018.
- H. Zhang, H. Chen, C. Xiao, S. Gowal, R. Stanforth, B. Li, D. Boning, and C.-J. Hsieh. Towards stable and efficient training of verifiably robust neural networks. *arXiv preprint arXiv:1906.06316*, 2019a.
- H. Zhang, Y. Yu, J. Jiao, E. Xing, L. E. Ghaoui, and M. Jordan. Theoretically principled trade-off between robustness and accuracy. In K. Chaudhuri and R. Salakhutdinov, editors, *Proceedings of the 36th International Conference on Machine Learning*, volume 97 of *Proceedings of Machine Learning Research*, pages 7472–7482. PMLR, 09–15 Jun 2019b.
- B. Zhao and H. Bilen. Dataset condensation with distribution matching. In *2023 IEEE/CVF Winter Conference on Applications of Computer Vision (WACV)*, pages 6503–6512, 2023. doi: 10.1109/WACV56688.2023.00645.
- B. Zhao, K. R. Mopuri, and H. Bilen. Dataset condensation with gradient matching. In *International Conference on Learning Representations*, 2021.



## A Proofs

We restate the proposition and theorems before presenting the proof for convenience.

### A.1 Proof for Proposition 4.3

**Proposition.** *The following statements are equivalent:*

- (1)  $\mathcal{S}^*$  is an  $\eta$ -MFC of  $\mathcal{T}$ ;
- (2)  $\mathcal{S}^* \in \arg \min_{\mathcal{S}} \{k : d_H(\mathcal{T}, \mathcal{S}) = \eta, |\mathcal{S}| = k\}$ .

*Proof.* Suppose  $\mathcal{S}^*$  is an  $\eta$ -MFC of  $\mathcal{T}$ , and  $\mathcal{S}_H^*$  is a minimizer of  $\min_{\mathcal{S}} \{k : d_H(\mathcal{T}, \mathcal{S}) = \eta, |\mathcal{S}| = k\}$ . We only need to prove  $|\mathcal{S}^*| = |\mathcal{S}_H^*|$ . Indeed, any dataset  $\mathcal{S}$  satisfying  $d_H(\mathcal{T}, \mathcal{S}) = \eta$  also satisfies  $d(\mathcal{T} \rightarrow \mathcal{S}) \leq \eta$ , hence  $|\mathcal{S}^*| \leq |\mathcal{S}_H^*|$ . If  $|\mathcal{S}^*| < |\mathcal{S}_H^*|$ , then we have  $d(\mathcal{S}^* \rightarrow \mathcal{T}) > \eta$ . By definition, there exists  $\mathbf{x}^* \in \mathcal{S}^*$  such that  $d(\mathbf{x}^*, \mathbf{y}) > \eta$  for all  $\mathbf{y} \in \mathcal{T}$ . However, this means by removing point  $\mathbf{x}^*$  from  $\mathcal{S}^*$ , the set  $\mathcal{S}^* \setminus \{\mathbf{x}^*\}$  is also a finite covering of  $\mathcal{T}$  with radius  $\eta$  and size  $|\mathcal{S}^*| - 1$ , which contradicts the minimality of  $|\mathcal{S}^*|$ .  $\square$

### A.2 Proof for Theorem 4.4

**Theorem.** *For a given dataset  $\mathcal{T} = \{\mathbf{x}_i\}_{i=1}^N$ , define the adjacency matrix of  $\mathcal{T}$  w.r.t. radius  $\eta$  as*

$$\mathbf{A}(\eta) := [a_{ij}(\eta)], \quad a_{ij}(\eta) = \begin{cases} 1, & \text{if } d(\mathbf{x}_i, \mathbf{x}_j) \leq \eta; \\ 0, & \text{otherwise.} \end{cases}$$

- (1) *The  $\eta$ -MCS of  $\mathcal{T}$  is one of the minimizers of*

$$\min_{\mathbf{s} \in \{0,1\}^N} \{\|\mathbf{s}\|_1 : \mathbf{A}(\eta) \cdot \mathbf{s} \geq \mathbf{1}\}; \quad (\eta\text{-MCS})$$

- (2) *The  $k$ -MCS of  $\mathcal{T}$  is one of the minimizers of*

$$\min_{\eta, \mathbf{s} \in \{0,1\}^N} \{\eta : \mathbf{A}(\eta) \cdot \mathbf{s} \geq \mathbf{1}, \|\mathbf{s}\|_1 = k\}. \quad (k\text{-MCS})$$

*Proof.* (1) By the first part of Definition 4.1, an  $\eta$ -MFC of  $\mathcal{T}$  is one of the minimizers of

$$\begin{aligned} & \min_{\mathcal{S}} \{k : d(\mathcal{T} \rightarrow \mathcal{S}) = \eta, |\mathcal{S}| = k\} \\ &= \min_{\mathcal{S}} \{|\mathcal{S}| : \sup_{\mathbf{x} \in \mathcal{T}} \inf_{\mathbf{y} \in \mathcal{S}} d(\mathbf{x}, \mathbf{y}) = \eta\} \\ &= \min_{\mathcal{S}} \{|\mathcal{S}| : \forall \mathbf{x} \in \mathcal{T}, \exists \mathbf{y} \in \mathcal{S}, d(\mathbf{x}, \mathbf{y}) \leq \eta\} \\ &= \min_{\mathcal{S}} \{|\mathcal{S}| : \forall \mathbf{x} \in \mathcal{T}, |\mathcal{S}_{\mathbf{x}}| \geq 1\} \end{aligned} \quad (3)$$

where  $\mathcal{S}_{\mathbf{x}} = \{\mathbf{y} \in \mathcal{S} : d(\mathbf{x}, \mathbf{y}) \leq \eta\} \subseteq \mathcal{S}$  for  $\mathbf{x} \in \mathcal{T}$ . Denote by  $\mathbf{A}_{\mathcal{T}, \mathcal{S}}(\eta)$  the adjacency matrix

$$\mathbf{A}_{\mathcal{T}, \mathcal{S}}(\eta) := [a_{\mathbf{x}, \mathbf{y}}(\eta)], \quad a_{\mathbf{x}, \mathbf{y}}(\eta) = \begin{cases} 1, & \text{if } d(\mathbf{x}, \mathbf{y}) \leq \eta; \\ 0, & \text{otherwise.} \end{cases}$$

Then Equation (3) is equivalent to

$$\min_{\mathcal{S}} \{|\mathcal{S}| : \mathbf{A}_{\mathcal{T}, \mathcal{S}}(\eta) \cdot \mathbf{1}_{|\mathcal{S}|} \geq \mathbf{1}\}$$

where  $\mathbf{1}_{|\mathcal{S}|}$  is the vector of all ones of dimension  $|\mathcal{S}|$ , and the inequality is element-wise. This immediately concludes the proof if  $\mathcal{S}$  is a subset of  $\mathcal{T}$ .

- (2) By the second part of Definition 4.1, a  $k$ -MFC of  $\mathcal{T}$  is one of the minimizers of

$$\begin{aligned} & \min_{\mathcal{S}} \{\eta : d(\mathcal{T} \rightarrow \mathcal{S}) = \eta, |\mathcal{S}| = k\} \\ &= \min_{\mathcal{S}} \{\eta : \mathbf{A}_{\mathcal{T}, \mathcal{S}}(\eta) \cdot \mathbf{1}_{|\mathcal{S}|} \geq \mathbf{1}, |\mathcal{S}| = k\} \end{aligned} \quad (4)$$

where the equality is directly derived from the previous part.  $\square$

### A.3 Proof for Theorem 5.5

**Theorem.** Let  $\mathcal{T}$  and  $\mathcal{S}$  be as defined in Definition 5.4. Then  $\hat{L}_\varepsilon^{adv}(\theta, \mathcal{T}) \leq \hat{G}_{\varepsilon+\eta}^{adv}(\theta, \mathcal{S})$ .

*Proof.* Let  $\mathcal{T} = \{(\mathbf{x}_i, y_i)\}_{i=1}^N$  and  $\mathcal{S} = \{(\tilde{\mathbf{x}}_j, \tilde{y}_j)\}_{j=1}^M$ . Since  $\mathcal{S}$  is an  $\eta$ -MCS of  $\mathcal{T}$ , for every  $(\mathbf{x}_i, y_i) \in \mathcal{T}$ , there exists  $(\tilde{\mathbf{x}}_j, \tilde{y}_j) \in \mathcal{S}$  such that  $y_i = \tilde{y}_j$  and  $\mathbf{x}_i \in \mathcal{B}_\eta(\tilde{\mathbf{x}}_j)$ , hence  $\mathcal{B}_\varepsilon(\mathbf{x}_i) \subseteq \mathcal{B}_{\varepsilon+\eta}(\tilde{\mathbf{x}}_j)$ . For each  $j = 1, \dots, M$ , define index set  $I_j = \{i : \mathbf{x}_i \in \mathcal{B}_\eta(\tilde{\mathbf{x}}_j)\} \subseteq \{1, \dots, N\}$ . By definition of adversarial loss over  $\mathcal{T}$ ,

$$\begin{aligned}
 \hat{L}_\varepsilon^{adv}(\theta, \mathcal{T}) &= \mathbb{E}_{(\mathbf{x}, y) \sim \hat{\nu}_\mathcal{T}} \left[ \max_{\|\delta\| \leq \varepsilon} l(f_\theta(\mathbf{x} + \delta), y) \right] \\
 &= \frac{1}{N} \sum_{i=1}^N \max_{\|\delta\| \leq \varepsilon} l(f_\theta(\mathbf{x}_i + \delta), y_i) \\
 &= \frac{1}{N} \sum_{j=1}^M \sum_{i \in I_j} \max_{\|\delta\| \leq \varepsilon} l(f_\theta(\mathbf{x}_i + \delta), y_i) \\
 &\leq \frac{1}{N} \sum_{j=1}^M \sum_{i \in I_j} \max_{\|\delta\| \leq \varepsilon + \eta} l(f_\theta(\tilde{\mathbf{x}}_j + \delta), \tilde{y}_j) \\
 &= \frac{1}{N} \sum_{j=1}^M |I_j| \cdot \max_{\|\delta\| \leq \varepsilon + \eta} l(f_\theta(\tilde{\mathbf{x}}_j + \delta), \tilde{y}_j) \\
 &= \hat{G}_{\varepsilon+\eta}^{adv}(\theta, \mathcal{S}).
 \end{aligned}$$

We conclude the proof by letting  $q_{(\mathbf{x}_j, y_j)} = |I_j|$ . □

## B Additional Results

### B.1 Visualization of “DIKU” dataset and its finite covering

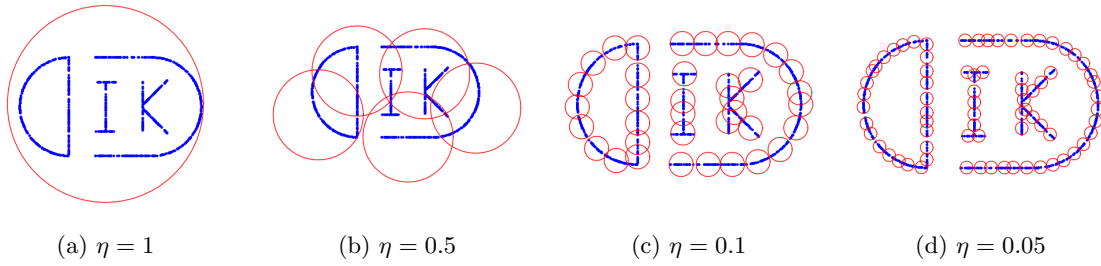


Figure 4: “DIKU” dataset and its  $\eta$ -MCS for different  $\eta$  values.

### B.2 Visualization of classical and generalized adversarial training over MCS of “DIKU” dataset

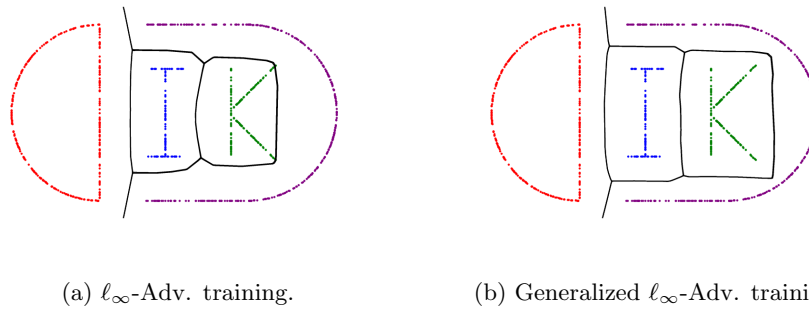


Figure 5: Visualization of the DIKU toy dataset and decision boundaries of models trained using 0.05-MCS. Figures from left to right are classical and generalized adversarial training respectively. The decision boundary between “K” and “U” (the right vertical line) clearly exemplifies the influence of generalized adversarial training.

### B.3 Training details

Table 3: Hyperparameters of standard and (generalized) adversarial training over coresets of “DIKU”, MNIST and CIFAR10 datasets. The considered coresets are **RAW**, **MCS**, **RAND**, and **DM**. The parameter  $\alpha$  is the step size in PGD attack. We see that the learning rate for MCS is much smaller than others, which is a quite interesting for future work to explain it in theory.

DATASET	CORESET	STD-LR	ADV-LR	$\alpha$
“DIKU”	RAW	$10^{-2}$	$10^{-3}$	$10^{-1}$
	MCS	$10^{-2}$	$10^{-3}$	
MNIST	RAW, RAND, DM	$10^{-3}$	$10^{-4}$	$10^{-1}$
	MCS	$10^{-3}$	$10^{-4}$	
CIFAR10	RAW, RAND, DM	$10^{-4}$	$10^{-5}$	$10^{-2}$
	MCS	$10^{-4}$	$10^{-5}$	

## B.4 Downstream performance of MCS w.r.t. $\ell_\infty$ -norm

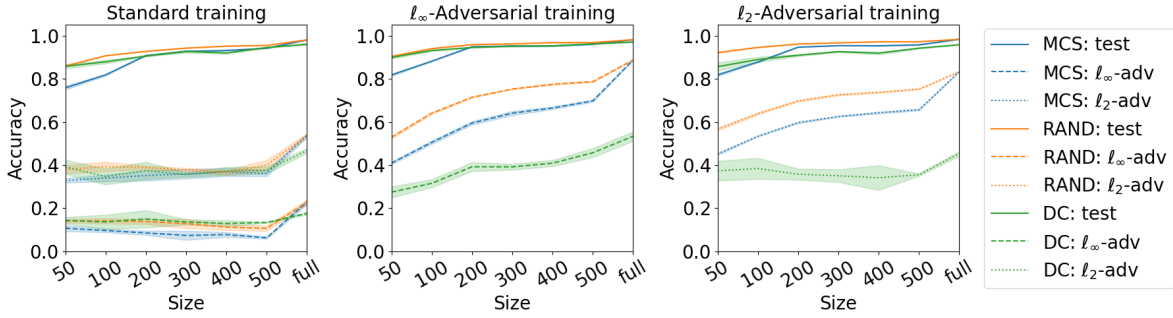


Figure 6: Performance of standard and robust models trained over different compressed dataset from MNIST. The figures from left to right are standard training,  $\ell_\infty$ - and  $\ell_2$ - adversarial training. The blue, orange and green lines stand for **MCS**, **RAND**, and **DM** respectively. Here MCSs are obtained by solving ( $\eta$ -MCS) w.r.t.  $\ell_\infty$ -norm. The solid, dashed and dotted lines stand for test,  $\ell_\infty$ - and  $\ell_2$ -robust accuracy respectively. In the horizontal axis, “full” means the original dataset for **MCS** and **RAND**, and  $k = 5000$  for **DM**.

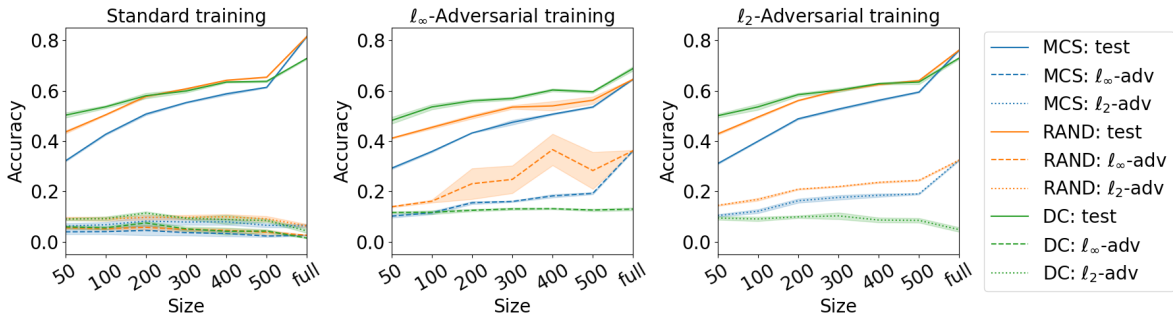


Figure 7: Performance of standard and robust models trained over different compressed dataset from CIFAR10. The figures from left to right are standard training,  $\ell_\infty$ - and  $\ell_2$ - adversarial training. The blue, orange and green lines stand for **MCS**, **RAND**, and **DM** respectively. Here MCSs are obtained by solving ( $\eta$ -MCS) w.r.t.  $\ell_\infty$ -norm. The solid, dashed and dotted lines stand for test,  $\ell_\infty$ - and  $\ell_2$ -robust accuracy respectively. In the horizontal axis, “full” means the original dataset for **MCS** and **RAND**, and  $k = 4000$  for **DM**.

## B.5 Comparison with classical and generalized adversarial training over MCS w.r.t. $\ell_\infty$ -norm

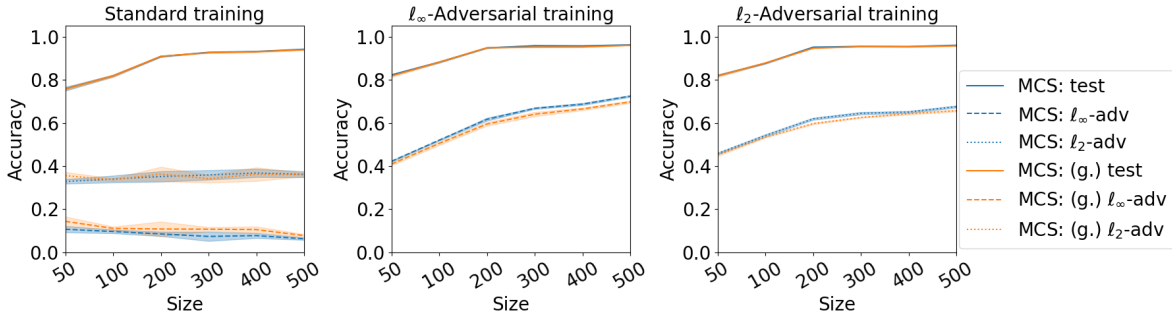


Figure 8: Comparison of classical and generalized adversarial training over MCS of MNIST dataset. Here MCSs are obtained by solving ( $\eta$ -MCS) w.r.t.  $\ell_\infty$ -norm. The figures from left to right are standard training,  $\ell_\infty$ - and  $\ell_2$ - adversarial training. The blue and orange lines stand for classical and generalized training respectively. The solid, dashed and dotted lines stand for test,  $\ell_\infty$ - and  $\ell_2$ - robust accuracy respectively.

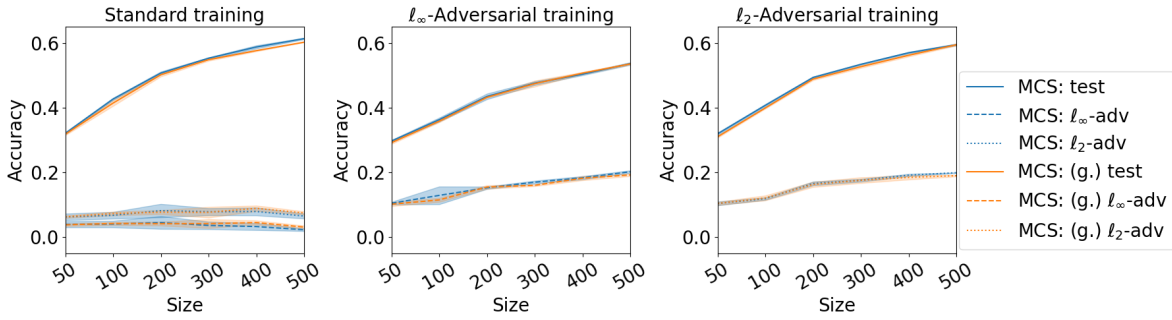


Figure 9: Comparison of classical and generalized adversarial training over MCS of CIFAR10 dataset. Here MCSs are obtained by solving ( $\eta$ -MCS) w.r.t.  $\ell_\infty$ -norm. The figures from left to right are standard training,  $\ell_\infty$ - and  $\ell_2$ - adversarial training. The blue and orange lines stand for classical and generalized training respectively. The solid, dashed and dotted lines stand for test,  $\ell_\infty$ - and  $\ell_2$ - robust accuracy respectively.

## B.6 Comparison with classical and generalized adversarial training w.r.t. $\ell_2$ -norm

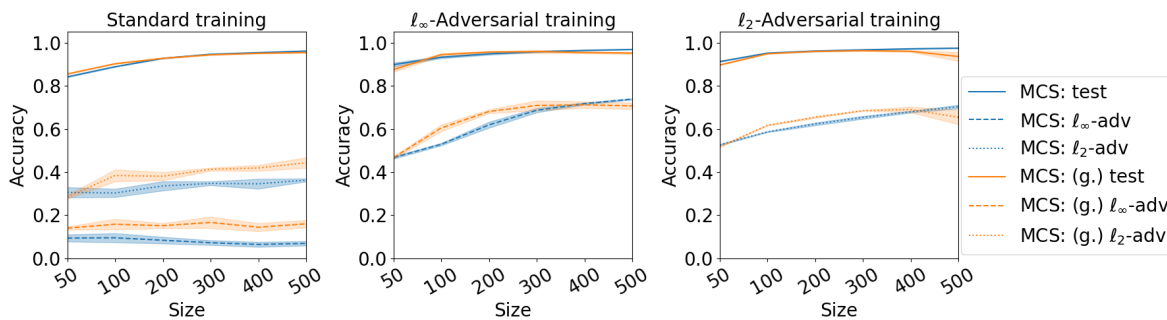


Figure 10: Comparison of classical and generalized adversarial training over MCS of MNIST dataset. Here MCSs are obtained by solving ( $\eta$ -MCS) w.r.t.  $\ell_2$ -norm. The figures from left to right are standard training,  $\ell_\infty$ - and  $\ell_2$ - adversarial training. The blue and orange lines stand for classical and generalized training respectively. The solid, dashed and dotted lines stand for test,  $\ell_\infty$ - and  $\ell_2$ - robust accuracy respectively.

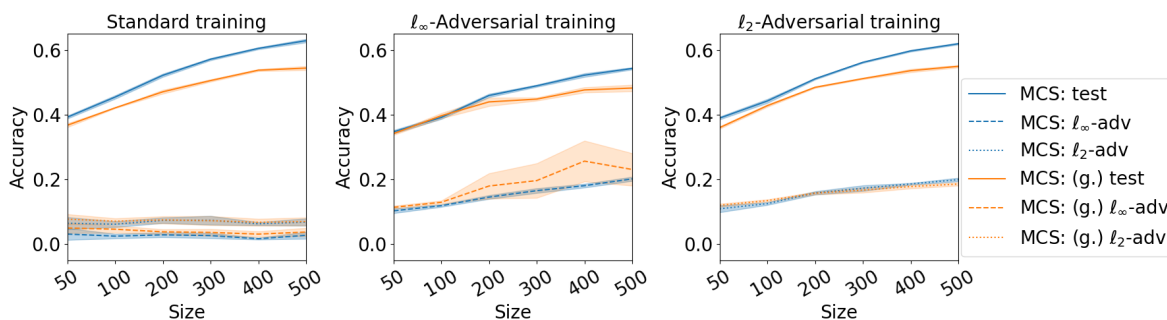


Figure 11: Comparison of classical and generalized adversarial training over MCS of CIFAR10 dataset. Here MCSs are obtained by solving ( $\eta$ -MCS) w.r.t.  $\ell_2$ -norm. The figures from left to right are standard training,  $\ell_\infty$ - and  $\ell_2$ - adversarial training. The blue and orange lines stand for classical and generalized training respectively. The solid, dashed and dotted lines stand for test,  $\ell_\infty$ - and  $\ell_2$ - robust accuracy respectively.